Available online at www.sciencedirect.com
SCIENCE DIRECT®
Journal of Solid State Chemistry 178 (2005) 950–955
JOURNAL OF SOLID STATE CHEMISTRY
www.elsevier.com/locate/jssc

Low-temperature synthesis and growth mechanism of uniform nanorods of bismuth sulfide

Zhaoping Liu, Dan Xu, Jianbo Liang, Wanjuan Lin, Weichao Yu, Yitai Qian*

Structure Research Laboratory and Department of Chemistry, University of Science and Technology of China, Hefei, Anhui 230026 China

Abstract

A low-temperature solution-phase method has been demonstrated for the synthesis of uniform nanorods of Bi_2S_3 with diameter of 18 nm and length of below 200 nm. Transmission electron microscopy (TEM), selected-area electron diffraction (SAED), and X-ray diffraction (XRD) studies revealed that these nanorods were grown from a colloidal dispersion of amorphous Bi_2S_3 particles, which was first formed through a thermal reaction between Bi-thiol complexes $Bi(SC_{12})_3$ and thioacetamide (TAA) in a pure dodecanethiol ($C_{12}SH$) solvent at a temperature of 95 °C. Based on these studies, the growth mechanism of Bi_2S_3 nanorods was properly proposed.

Keywords: A1. Crystal morphology; Nanostructure; A2. Crystal growth; B1. Nanomaterials

1. Introduction

Bismuth sulfide (Bi_2S_3) is a direct band gap material with E_g of 1.3 eV, which makes it a useful material for photodiode arrays and photovoltaic converters [1]. It also belongs to a family of solid-state materials with applications in thermoelectric cooling technologies based on the Peltier effect [2]. Furthermore, the availability of Bi_2S_3 nanostructures should be able to bring in new types of applications or to enhance the performance of the currently existing device as a result of quantum size effects. For example, nanostructured thin film of Bi_2S_3 was found to have a great improvement in photoelectrochemical cell performance due to their size quantization effects [3].

The size and shape of nanostructures are two crucial factors in determining the properties of nanomaterials, and thus the artificial control of size and shape is of great interest [4]. One-dimensional (1D) nanostructures of Bi_2S_3 have been synthesized by various solution-based synthetic schemes including the most popular solvothermal/hydrothermal process [5]. However, the nanorods (nanowires, or nanoribbons) prepared through these procedures usually had large lateral dimensions (usually tens of nanometers) [5a–g], exhibiting no quantum size effects. Thus the present challenge is to produce high-quality 1D nanostructures with a small lateral dimension lower than the exciton Bohr radius of Bi_2S_3 semiconductor at a relatively low temperature. It was also noted that, when a surfactant exsited in the synthetic system, the produced Bi_2S_3 nanorods often had a properly decreased size [5h–j]. The size control of nanostructures by using surfactants was believed to result from the chemical absorption of surfactant molecules on the surfaces of the growing nanoparticles [6]. Therefore, a suitable surfactant, which has a strong absorption on the crystalline faces of Bi_2S_3, is expected to be used for the synthesis of Bi_2S_3 nanorods with small sizes.

In this paper, we demonstrate a simple and mild solution-phase route to the synthesis of uniform nanorods of Bi_2S_3 have a typical diameter of 18 nm. The synthesis was performed with bismuth oxide (Bi_2O_3) and thioacetamide (TAA) as the reagents and surfactant

*Corresponding author. Tel.: +86-551-3603204; fax: +86-551-3607402.
E-mail address: ytqian@ustc.edu.cn (Y. Qian).

0022-4596/$ - see front matter © 2004 Elsevier Inc. All rights reserved.
doi:10.1016/j.jssc.2004.06.043

dodecanethiol ($C_{12}SH$) as the solvent at a temperature as low as 95 °C. The chemical reactions involved in the entire synthesis could be formulated as following Eqs. (1)–(3):[7]

$$Bi_2O_3 + 6C_{12}SH \xrightarrow{C_{12}SH} 2Bi(SC_{12})_3 + 3H_2O \quad (1)$$

$$CH_3CSNH_2 \xrightarrow{C_{12}SH} CH_3CN + H_2S \quad (2)$$

$$2Bi(SC_{12})_3 + 3H_2S \xrightarrow{C_{12}SH} Bi_2S_3 + 6C_{12}SH \quad (3)$$

In this synthesis, $C_{12}SH$ was served as both the coordinating solvent and the surfactant. The formation process of Bi_2S_3 nanorods has been systemically investigated herein.

2. Experimental section

All chemicals were of analytical grade and were purchased from Shanghai Chemical Reagents Company. Bi_2S_3 nanorods were synthesized by the thermal reaction between Bi-thiolate complexes ($Bi(SC_{12})_3$) and TAA in $C_{12}SH$ solvent. In a typical procedure, Bi_2O_3 (1 mmol, 0.466 g) was added into 7.5 mL of $C_{12}SH$ at 95 °C. A clear and orange-colored solution formed soon, indicative of the formation of Bi-thiolate complexes. In another vessel, 3 mmol of TAA was dissolved in 7.5 mL of $C_{12}SH$ at 95 °C, and then this hot solution was injected into the $Bi(SC_{12})_3$ solution under vigorous stirring. The resulting colloidal solution was further aged at 95 °C without stirring. The crystal growth was monitored by sampling small portions of the reaction mixture at various aging periods. The extracted solution was quenched to room temperature by adding about 10 mL of ethanol. The solid samples was collected by centrifugation, washed with ethanol several times to remove the excess $C_{12}SH$ and other impurities, and then dried in a vacuum oven at 60 °C for 4 h.

The transmission electron microscopy (TEM) images and selected-area electron diffraction (SAED) were captured on a Hitachi Model H-800 instrument at an acceleration voltage of 200 kV. High-resolution TEM (HRTEM) images, SAED patterns, and the energy-dispersed X-ray spectrometry (EDS) were obtained on a JEOL-2010 transmission electron microscopy at an acceleration voltage of 200 kV. The X-ray diffraction (XRD) analysis was performed using a Philip X' Pert PRO SUPER γA rotation anode with Ni-filtered Cu Kα radiation ($\lambda = 1.54178$ Å). Fourier transform Infrared absorption (FTIR) spectra were obtained with a Shimadzu IR-440 spectrometer at room temperature.

3. Results and discussion

The Bi_2S_3 nanostructures at various stages of the growth process were characterized using TEM, SAED and XRD. Fig. 1 shows images of the samples that were taken from the reaction mixture after mixing for 1, 5, 10, 30 min, 2 h, and 10 h. These images clearly show the evolution of Bi_2S_3 nanostructures from aggregated nanoparticles to thin nanofibers, and finally to thicker nanorods over time at 95 °C. Once the TAA solution was added into the $Bi(SC_{12})_3$ solution, a dark brown

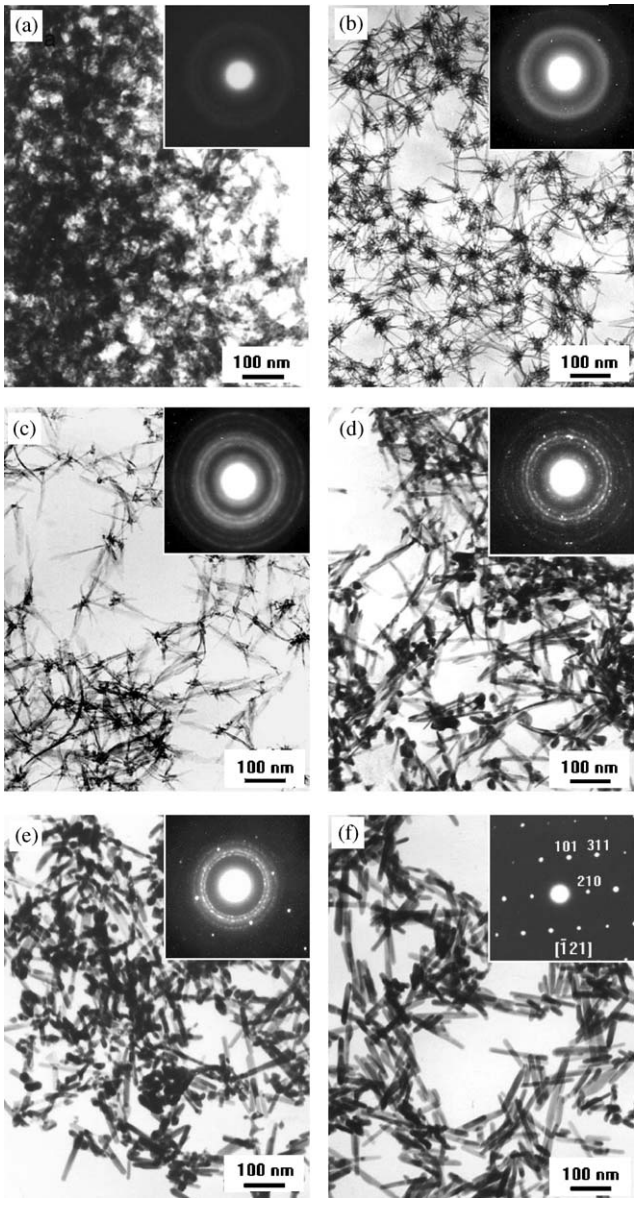

Fig. 1. TEM images of six samples, showing different growth stages of Bi_2S_3 nanorods. These samples were taken from the reaction mixture after aging for (a) 1 min, (b) 5 min, (c) 10 min, (d) 30 min, (e) 2 h, and (e) 10 h, respectively. Insets: SAED patterns of these samples, indicating an increased crystallinity of the products with the elongation of aging periods.

colloidal solution formed rapidly, suggesting the formation of Bi_2S_3 nanoparticles. Fig. 1a shows the TEM images of the sample taken from the mixture after only 1 min of aging. This image demonstrates that the initial products are predominated by aggregated nanoparticles. These aggregates were amorphous and did not produce any SAED pattern, as shown in the inset of Fig. 1a. XRD analysis (see curve a of Fig. 2) further confirms that the initial products are amorphous. After 5 min of aging, a large amount of fibrillar nanostructures had formed dramatically, and these nanofibers seemed to emanate from one center and grow in all directions thus forming 3D spherical nanoflower patterns (see Fig. 1b). These nanofibers had a uniform diameter of just 3–4 nm and length up to 100 nm, and they all have cone-shaped tips; the center of nucleation (core) had a diameter of about 30 nm. Both the SAED (inset of Fig. 1b) and XRD patterns (curve b of Fig. 2) reveal that the nanoflowers are still poorly crystalline, indicating that each of them had a large and amorphous core. It could be believed that the nucleation of crystalline Bi_2S_3 had randomly occurred on the surfaces of the amorphous aggregates and the growth of nanofibers was based on the consumption of amorphous particles. It was found that the fibers of nanoflowers became thicker and longer and their cores were diminished in subsequent several minutes. The TEM image of the 10-min product is shown in Fig. 1c, demonstrating that the nanofibers are 5–6 nm thick and 100–150 nm long and the sizes of cores are reduced to 15–20 nm. Both the SAED (inset of Fig. 1c) and XRD patterns (curve c of Fig. 2) show that these nanoflowers have a increased crystallinity, agreeing with the decreased ratio of amorphous cores to crystalline nanofibers. Further observations showed that the nanofibers began to rupture from their cores after over 10-min aging and they further developed into nanorods with larger diameters and lower aspect ratios. These nanoflowers were completely broken into independent nanofibers/nanorods and nanoparticles (from the original cores) after about 30-min aging (see Fig. 1d). These nanofibers (or nanorods) had diameters of 5–10 nm and lengths of 100–200 nm, and the nanoparticles were 15–20 nm sizes. The inset of Fig. 1d shows the SAED pattern taken from a random aggregate of these nanorods and nanoparticles. In this pattern, several high-intensity differaction rings can be observed, and these concentric rings can all be assigned to the orthorhombic phase of Bi_2S_3. The XRD pattern (Fig. 2d) also exhibits many identified diffraction peaks of Bi_2S_3, indicative of the further increased crystallinity of these nanostructures. With the elongation of aging time, the thin and flexible nanofibers would develop into the thicker and straight nanorods, and the coexisted nanoparticles would progressly disappear. After 2 h, nanorods formed with a uniform diameter of 12 nm (see Fig. 1e); after 5 h, the diameter of nanorods was increased to 15 nm, and a small amount of nanoparticles still coexisted. Forming nearly pure nanorods could take about 10 h of aging. As illustrated in Fig. 1f, the 10-h products consisted of independent nanorods with a uniform diameter of 18 nm and length of 150–200 nm; all the nanorods had distinctly rounded ends, suggesting a ripenning process had occured. Almost no small particles were detected. Further extending the aging time did not remarkably increase the nanorod sizes. For example, the diameter of nanorods was slightly increased to ~20 nm after 24 h of aging, indicative of a much slow rate of nanorod growth in the latter process. From the XRD patterns (Fig. 2a–f) and SAED patterns (insets of Fig. 1a–f), one can see that the products had an increased crystallinity with the elongation of the aging periods.

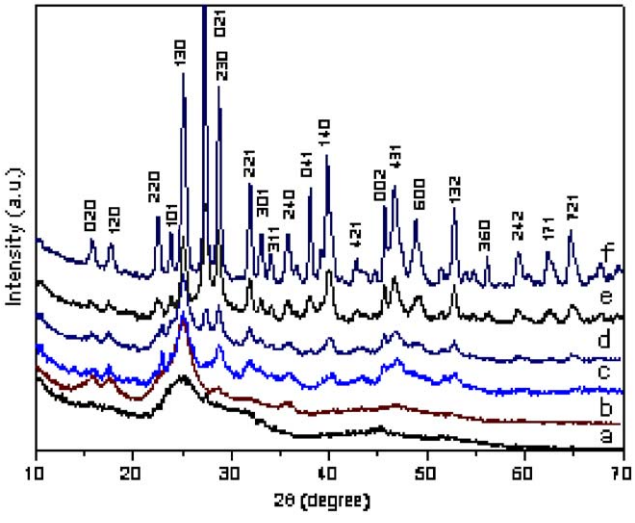

Fig. 2. XRD patterns of the same samples as shown in Fig. 1a–f.

Based on the above experimental results observed, it could be concluded that the formation of Bi_2S_3 nanorods involved at least five distinctive stages: (i) the formation of large aggregates of amorphous Bi_2S_3 nanoparticles in the initial 1 min of the reaction, (ii) the rapid nucleation and growth of Bi_2S_3 nanofibers on the surfaces of amorphous aggregates, resulting in the formation of nanoflowers, (iii) the continous growth of nanofibers at the expense of their amorphous supports, (iv) the rupture of nanoflowers, generating independent nanofibers/nanorods and nanoparticles, and (v) the formation of uniform nanorods. Such a formation process of Bi_2S_3 nanorods is depicted schematically in Fig. 3. In the early stage (1–10 min), amorphous particles could dissolve into the solution and server as the 'food' for the growth of nanofibers, because they had a higher free energy relative to the crystallites. This spontaneous process continued until all amorphous particles had been depleted in the solution, leaving behind nanoflowers with very small cores. In this growth

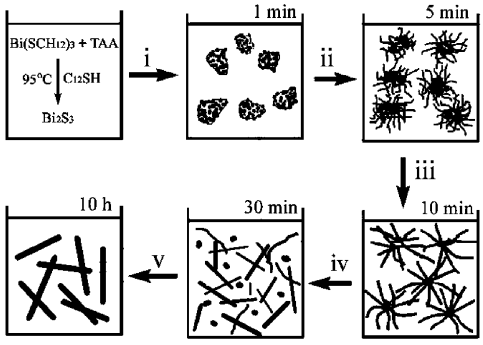

Fig. 3. Schematic illustration of a formation process for Bi_2S_3 nanorods, which could be rationally supported by TEM studies given in Fig. 1.

stage, the crystal growth mainly occurred in their long axis as evidenced by the fast increase of lengths and little increase of diameters. This is similar to that of CdSe nanorods that Peng and coworkers have observed, strongly suggesting that the growth of nanofibers is also a diffusion-controlled process [8]. At the same time, a crystallization process might also occured in the cores of nanoflowers, resulting in crystalline cores. When the cores had sizes near to the lateral dimensions of nanofibers, the possible presence of strain could lead to the rupture of nanoflowers. After rupturing, three forms of nanostructures (nanofibers, nanorods, and nanoparticles) coexisted in the colloidal solution. When this colloidal dispersion was continuously heated at 95 °C, the small nanoparticles would spontaneously dissolved into the solution due to a relativly higher free energy comparing to nanorods; at the same time, the growth units in the solution would diffuse onto the high-energy surface of the growing nanorods. As a result, uniform nanorods would form eventually. Obviously, the growth of nanorods is a typical Ostwald ripening process [9], but this ripening process has spended a much long period (up to 10 h) and the crystal growth focused on the short axis as observed by TEM.

We also have characterized the as-synthesized Bi_2S_3 nanorods (10-h products) using HRTEM, SAED, and EDS. Shown in Fig. 4a is a high-magnification TEM image of several nanorods, in which the distinctly rounded ends can be clearly identified. The inset of Fig. 4a exhibits a typical SAED pattern that was recorded from rod A; it can be indexed to be the [010] zone axis of orthorhombic Bi_2S_3. These diffraction spots demonstrate the single crystallinity of this nanorod. The corresponding HRTEM image (Fig. 4b) shows two set of distinct fringe spacings of ca. 5.5 and 3.7 Å (also cleary shown in the inset of Fig. 4b) that agree well with the separation between the (200) and (101) lattice planes of orthorhombic Bi_2S_3, respectively. Fig. 4c shows a HRTEM image of the tip of rod B. the regular spacing of the observed lattice planes was ca. 7.9 Å, which is

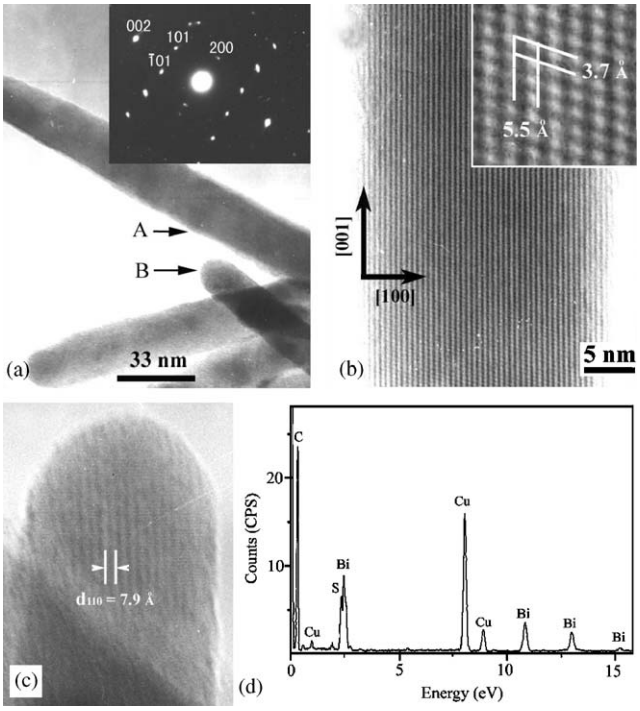

Fig. 4. (a) High-magnification TEM image of Bi_2S_3 nanorods prepared after 10 h of aging; the inset is a SAED pattern taken on nanorod A, which is indexed to be the [010] of orthorhombic Bi_2S_3. (b) corresponding HRTEM image of nanorod A; the inset gives an enlarged view of the HRTEM image. (c) HRTEM image of nanorod B. (d) corresponding EDS pattern taken on the nanorods.

consistent with the separation of (110) planes of Bi_2S_3. These results indicate that the as-prepared nanorods are structurally uniform single crystals with a growth direction of [001] (*c*-axis).

The composition of the nanorods as calculated from the EDS spectrum (Fig. 4d) gives a Bi:S atomic ratio of 1:1.66. The excess of S with respect to stoichiometry in the nanorods may attribute to the abundant dodecanethiol adsorbing on the surfaces of nanorods. Furthermore, this sample was characterized by FTIR. Fig. 5 shows the FTIR spectra of the 10-h products and the free $C_{12}SH$. The similarity of the two spectra indicates the $C_{12}SH$ molecules have indeed become a part of the products. Since our HRTEM studies suggested that these is no possibility of the intercalation of $C_{12}SH$ molecules in the nanorods, and $C_{12}SH$ molecules are the strong ligands for Bi(III), it could be believed that the as-prepared nanorods were heavily coated by $C_{12}SH$ molecules on their surfaces according to the indirect evidences from both the EDS and FTIR spectra. Moreover, the remarkable difference in the peak intensity between the two spectra implies that the absorbing $C_{12}SH$ molecules form a relatively close-packed layer and thus molecular motion is constrained [10]. The peak, corresponding to the C-S stretching mode ($\nu_{C-S} = 721\,cm^{-1}$), is hardly observed in curve a

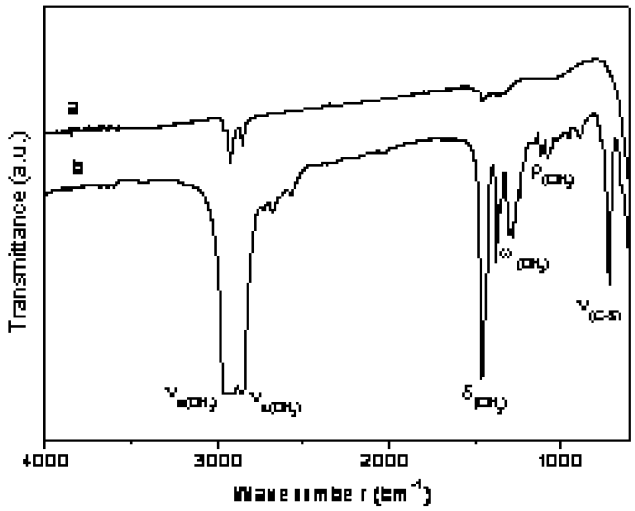

Fig. 5. FTIR spectra of (a) Bi_2S_3 nanorods and (b) free $C_{12}SH$.

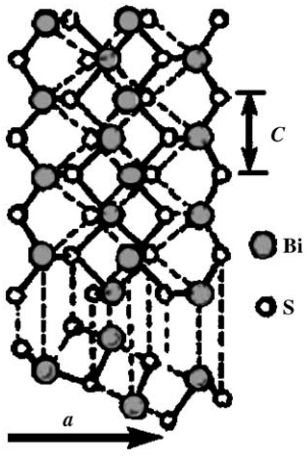

Fig. 6. The [010] projection of the atomic arrangements for orthorhombic Bi_2S_3, showing a lamellar structure with linked Bi_2S_3 units forming infinite chains parallel to the *c*-axis.

of Fig. 5, suggesting that the S-Bi bonds have been formed between the thiol molecules and the surface Bi atoms.

The growth of Bi_2S_3 nanofibers or nanorods with a preferential direction of *c*-axis can be ascribed to its particular structure. Bi_2S_3 has a lamellar structure with linked Bi_2S_3 units forming infinite chains parallel to the *c*-axis [11], as illustrated in Fig. 6. The stronger covalent bond between the planes perpendicular to *c*-axis facilitates higher growth rate along *c*-axis. In principle, relatively long 1D nanostructures of Bi_2S_3 should form due to its highly anisotropic structure. As reported previously, 1D nanostructures of Bi_2S_3 prepared by a solvothermal/hydrothermal method ususally had lengths up to several micrometers, sometimes even to millimeter scale [5]. Why did our present process only produce Bi_2S_3 nanorods with such small sizes? We believed that there are two reasons that may be responsible for this. First, a bursting nucleation had occurred on the surfaces of amorphous aggregates of Bi_2S_3. This process resulted in forming numerous seeds, favoring for the formation of small-sized nanostructures [12]. Second, the present synthesis was performed in a coordinating solvent ($C_{12}SH$). The use of coordinating solvents to control the shapes and sizes of semiconductor chalcogenide nanostructures has been extensively explored in previous studies [13]. It is generally accepted that the coordinating solvent molecules kinetically controls the growth rates of various faces of the growing nanocrystals through selective adsorption and desorption on these surfaces. In present case, a mass of $C_{12}SH$ molecules could chemically adsorb on the surfaces of the growing particles through a strong S-Bi bonding. The protective effect of $C_{12}SH$ would result in significantly decreasing the grow rates of all different crystalline faces. Especially the growth along *c*-axis was largely confined. As a result, the Bi_2S_3 1D nanostructures formed even after 24 h of aging still had a limited length (<200 nm) and a small lateral dimension (<20 nm).

4. Conclusion

In summary, uniform nanorods of Bi_2S_3 have been synthesized by the thermal reaction between Bi-thiol complexes $Bi(SC_{12})_3$ and TAA in $C_{12}SH$ solvent at 95 °C. The nanorods formed after 10-h aging were just 18 nm in diameter and below 200 nm in length. In this soft-solution process, the evolution of Bi_2S_3 nanostructures over time had undergone five stages with characteristic forms: amorphous particles, nanoflowers with very thin nanofibers and large cores, nanoflowers with small cores, mixture of nanofibers/nanorods and nanoparticles, and uniform nanorods. The growth of Bi_2S_3 nanorods with such small sizes could be ascribed to two important factors: one is the rapid nucleation, resulting in the formation of numerous seeds with extremely small sizes; the other is the protective effect of $C_{12}SH$ absorbing on the surfaces of the growing particles, leading to the decrease of the growth rate along all directions, especially [001] direction. The synthesis method developed in the present study has several advantages: the synthetic process uses inexpensive and nontoxic regents such as metal oxides and thioacetamide, the reaction conditions are mild and simple, and the present method may be extended to prepare uniform and small-size nanostructures of various sulfides because $C_{12}SH$ molecules are very effective ligands for various species. In fact, monodisperse nanocrystals of various sulfides have been prepared successfully by this feasible method and will be reported elsewhere.

Acknowledgement

Financial support from the National Nature Science Foundation of China and the 973 Project of China are appreciated.

References

[1] (a) D.D. Miller, A. Heller, Nature (London) 262 (1976) 280;
(b) J.M. Schoijet, Sol. Energy Mater. 1 (1979) 43;
(c) P.K. Mahapatra, C.B. Roy, Sol. Cells 7 (1982/83) 225;
(d) M.E. Rincón, R. Suárez, P.K. Nair, J. Phys. Chem. Solids 57 (1996) 1947.
[2] P. Boudjouk, M.P. Remngton Jr., D.G. Grier, B.R. Jarabek, G.J. McCarthy, Inorg. Chem. 37 (1998) 3538.
[3] (a) R. Suarea, P.K. Nair, P.V. Kamat, Langmuir 14 (1998) 3236;
(b) R.S. Mane, B.R. Sankapal, C.D. Lokhande, Mater. Chem. Phys. 60 (1999) 196.
[4] (a) J. Hu, T.W. Odom, C.M. Lieber, Acc. Chem. Res. 32 (1999) 435;
(b) Z. Zhang, X. Sun, M.S. Dresselhaus, J.Y. Ying, Phys. Rev. B 61 (2000) 4850;
(c) Z.L. Wang, Adv. Mater. 12 (2000) 1295;
(d) V.F. Puntes, K.M. Krishnan, A.P. Alivisatos, Science 291 (2001) 2115;
(e) Y.G. Sun, Y.N. Xia, Science 298 (2002) 2176.
[5] (a) S.H. Yu, Y.T. Qian, L. Shu, Y. Xie, L. Yang, C.S. Wang, Mater. Lett. 35 (1998) 116;
(b) W.X. Zhang, Z.H. Yang, X.M. Huang, S.Y. Zhang, W.C. Yu, Y.T. Qian, Y.B. Jia, G.E. Zhou, L. Chen, Solid State Commun 119 (2001) 143;
(c) D.B. Wang, M.W. Shao, D.B. Yu, G.P. Li, Y.T. Qian, J. Cryst. Growth 243 (2002) 331;
(d) G.Z. Sheng, D. Chen, K.B. Tang, F.Q. Li, Y.T. Qian, Chem. Phys. Lett. 370 (2003) 334;
(e) Y.W. Koh, C.S. Lai, A.Y. Du, E.R.T. Tiekink, K.P. Loh, Chem Mater 15 (2003) 4544;
(f) Z.P. Liu, S. Peng, Q. Xie, Z.K. Hu, Y. Yang, S.Y. Zhang, Y.T. Qian, Adv. Mater. 15 (2003) 936;
(g) Z.P. Liu, J.B. Liang, S. Li, S. Peng, Y.T. Qian, Chem. Eur. J. 10 (2004) 634;
(h) Q. Li, M.W. Shao, J. Wu, G.H. Yu, Y.T. Qian, Inorg. Chem. Commun. 5 (2002) 933;
(i) G.J. Xing, Z.J. Feng, G.H. Chen, W. Yao, X.M. Song, Mater. Lett. 57 (2003) 4555;
(j) Q. Lu, F. Gao, S. Komarneni, J. Am. Chem. Soc. 126 (2004) 54.
[6] (a) J.M. Petroski, Z.L. Wang, T.C. Green, M.A. El-Sayed, J. Phys. Chem. B 102 (1998) 3316;
(b) C.J. Johnson, E. Dujardin, S.A. Davis, C.J. Murphy, S. Mann, J. Mater. Chem. 12 (2002) 1765;
(c) Y.G. Sun, B. Mayers, T. Herricks, Y.N. Xia, Nano Lett 3 (2003) 955.
[7] (a) T.D. Sugimoto, C.E. Dirige, J. Colloid Interface Sci. 176 (1995) 442;
(b) Y. Zhou, H. Itoh, T. Uemura, K. Naka, Y. Chujo, Langmuir 18 (2002) 5287.
[8] Z.A. Peng, X. Peng, J. Am. Chem. Soc. 123 (2001) 1389.
[9] A.R. Roosen, W.C. Carter, Physica A 261 (1998) 232.
[10] S. He, J. Yao, P. Jiang, D. Shi, H. Zhang, S. Xie, S. Pang, H. Gao, Langmuir 17 (2001) 1571.
[11] J. Black, E.M. Conwell, L. Seigle, C.W. Spencer, J. Phys. Chem. Solids 2 (1957) 240.
[12] (a) Y.G. Sun, Y.D. Yin, B.T. Mayers, T. Herricks, Y.N. Xia, Chem. Mater. 14 (2002) 4736;
(b) E.V. Shevchenko, D.V. Talapin, H. Schnablegger, A. Kornowski, Ö. Festin, P. Svedlindh, M. Haase, H. Weller, J. Am. Chem. Soc. 125 (2003) 9090.
[13] (a) C.B. Murry, D.J. Norris, M.G. Bawendi, J. Am. Chem. Soc. 15 (1993) 8706;
(b) X. Peng, M.C. Schlamp, A. Kadavanich, A.P. Alivisatos, J. Am. Chem. Soc. 119 (1997) 7019;
(c) X. Peng, L. Manna, W. Yang, J. Wickham, E. Scher, A. Kadavanich, A.P. Alivisatos, Nature 404 (2000) 59;
(d) Y.W. Jun, S.M. Lee, N.J. Kang, J. Cheon, J. Am. Chem. Soc. 123 (2001) 5150;
(e) J. Joo, H.B. Na, T. Yu, J.H. Yu, Y.W. Kim, F. Wu, J.Z. Zhang, T. Hyeon, J. Am. Chem. Soc. 125 (2003) 11100.